

# High-Rate, Reliable Communications with Hybrid Space-Time Codes

Joaquín Cortez<sup>1</sup> and Miguel Bazdresch<sup>2</sup>

<sup>1</sup>*Instituto Tecnológico de Sonora*

<sup>2</sup>*Instituto Tecnológico de Estudios Superiores de Occidente  
México*

## 1. Introduction

Current wireless services and applications, such as third-generation (3G) cellular systems and Wi-Fi networks, offer capabilities far beyond what was previously available. With data rates on the order of 100kbit/s for mobile cellular users and up to 54Mbit/s on fixed WLANs, these systems provide attractive services such as internet access and video telephony.

In the near- and medium-term, however, it is expected that the capabilities of wireless networks will grow exponentially. The future of wireless applications and services will require high spectral efficiency, data rates on the order of 1Gbit/s, WLAN and WMAN integration and seamless connectivity, for devices ranging from a cell phone to a full-fledged desktop computer. Examples of services that will be available to users are Multimedia Messaging Service (MMS), HDTV-quality digital video, mobile TV, and Quality of Service guarantees.

The fulfillment of these promises hinges on several key telecommunications technologies. OFDM and related modulation techniques promise high spectral efficiency on wideband channels. For example, adaptive radio interfaces and cognitive radio will allow efficient spectrum use and smooth handoff between disparate networks. Software-defined radio and advanced circuit design techniques are needed to support all required functionality while meeting size, weight and power consumption requirements. All of these areas present heavy research activity.

Another key technology is known as multiple-input, multiple-output (MIMO) systems. These communications systems use multiple antennas at the transmitter and receiver, and have powerful capabilities in two respects: they can improve link reliability, and/or they can increase the data rate, without requiring extra power or bandwidth. Compared to more conventional systems, with only one antenna at the transmitter end (single-input multiple-output, SIMO), at the receiver end (multiple-input single-output, MISO), or at both ends (single-input single-output, SISO), MIMO systems offer additional (spatial) degrees of freedom (Tse & Viswanath, 2005), (Biglieri et al., 2007). While information-theoretic capacity analyses support the potential gains (and illustrate the limitations) offered by MIMO

systems (Telatar, 1999), (Foschini & Gans, 1998), practical coding strategies that take advantage of them must be devised.

Fig. 1. MIMO system transmit chain.

Assuming a narrowband channel and adequate antenna separation, MIMO systems allow signal coding over time (that is, over multiple symbol periods) and over space (using all the available antennas). A space-time code is a mapping from modulated symbols to  $n_t$  spatial data streams, each of which is transmitted by a different antenna. This process is illustrated in Figure 1. A data stream  $\mathbf{b}$  is interleaved and coded with a conventional FEC coder. The interleaved/coded stream  $\mathbf{c}$  is modulated, and the resulting stream  $\mathbf{x}$  is space-time coded. The space-time encoder takes  $R_s T$  symbols from  $\mathbf{x}$  at a time, and (linearly) maps it to space-time code matrix  $\mathbf{X}$ . Each column of  $\mathbf{X}$  is transmitted during a symbol period. If the transmitter has any channel-state information (CSI), then a beamformer may be used to allocate power in an optimal way among the transmitter antennas. We will assume no transmitter CSI, so that beamformer matrix  $\mathbf{W}$  is equal to the identity matrix. Matrix  $\mathbf{X}$  has dimensions  $n_t \times T$ , so that it takes  $T$  symbol periods to transmit  $R_s T$  symbols and the code rate is  $R_s$ . The set of all possible code matrices is the space-time code, and the design problem consists in finding a set that meets given performance criteria.

Assuming that the channel presents quasi-static Rayleigh fading (the channel remains constant during  $T$  symbol periods), and assuming there are  $n_r$  receiver antennas, then the channel may be modeled as a matrix  $\mathbf{H}$  of dimensions  $n_r \times n_t$ , where each element  $h_{i,j}$  is a complex Gaussian random variable with 0 mean and variance 1, and represents the channel coefficient from transmitter antenna  $j$  to receiver antenna  $i$ . Assuming perfect CSI at the receiver, the received matrix  $\mathbf{Y}$  may be written as

$$\mathbf{Y} = \mathbf{H}\mathbf{X} + \mathbf{Z}, \quad (1)$$

where matrix  $\mathbf{Z}$  corresponds to additive Gaussian white noise. Its entries are complex Gaussian random variables with 0 mean and variance  $N_0$ . If  $E_s$  is the signal energy transmitted for each antenna during each symbol period, then the signal-to-noise ratio (SNR) at the receiver is defined as

$$SNR = \frac{n_t E_s}{N_0}. \quad (2)$$

Under these conditions, we may identify three important code performance measures that characterize a given space-time code.

**Multiplexing gain.** Channel capacity  $C$ , or the achievable data rate assuming optimum coding and decoding, scales with  $\min(n_T, n_R)$ :

$$C(n_T, n_R, SNR) \sim \min(n_T, n_R) \log(SNR). \quad (3)$$

This means that increasing the number of antennas at either side allows an increase in data rate without increasing error probability. This may be interpreted as the separation of channel  $\mathbf{H}$  into a number of parallel, independent channels that do not interfere with each other. Equation (3) suggests that this separation is possible at the receiver side, so that, for a fixed error probability, the data rate may be increased by up to  $\min(n_T, n_R)$  bps/Hz for each 3dB increase in SNR. The increase in data rate afforded by a particular code is known as its multiplexing gain.

**Diversity gain.** Assuming code matrix  $\mathbf{C}$  is transmitted, an upper bound on the probability that the receiver instead decides in favor of code matrix  $\mathbf{D}$  has the form

$$K^{-n_R} J^{-m_R}, \quad (4)$$

where  $r$ ,  $K$  and  $J$  are real numbers that depend on the particular properties of the space-time code. In particular,  $r$  and  $K$  depend on the code matrices, while  $J$  depends on  $E_s$  and  $N_0$ . The number  $m_R$  is known as the diversity gain of the code, since it is the asymptotic negative slope of the error probability, in a log-log scale, as a function of SNR. The maximum achievable diversity gain is  $n_R n_T$ . This means that for a 3dB increase in SNR, the error probability decreases by  $2^{-n_R n_T}$ .

**Coding gain.** In Equation (4), the number  $K$  is known as the coding gain. It is independent of SNR, so it has no effect on the slope of the error probability. However, it is important to make it as large as possible to improve code performance.

Fig. 2. Coding gain and diversity gain.

Coding and diversity gains are illustrated in Figure (2). Consider three space-time codes, A, B, and C, with error performance as shown in Figure (2). Code B has a diversity gain over Code A; this can be seen as an improvement on the slope of its error probability as SNR increases. On the other hand, Codes B and C provide the same diversity; however, code C has a coding gain advantage over Code B.

It is not possible to maximize all gains at the same time (Zheng & Tse, 2003). In particular, there is a trade-off that must be made between multiplexing and diversity gains. If a space-time code has multiplexing gain  $R$ , then the maximum diversity gain it may achieve is given by

$$d(R) = (n_R - R)(n_T - R). \quad (5)$$

There has been a large research effort to design space-time codes that achieve the gains promised by information theory. In the rest of this chapter, we summarize some of these efforts, focusing on so-called hybrid codes.

## 2. Design of space-time codes

### 2.1 Early developments

Two of the first space-time codes are V-BLAST (Golden et al., 1999) and the Alamouti Scheme (Alamouti, 1998). V-BLAST is a purely spatial multiplexing code; the space-time coder is simply a serial-to-parallel converter. It maximizes data rate while offering relatively poor link reliability. In contrast, the Alamouti Scheme is a pure diversity scheme; its data rate is the same as a SISO system but it offers maximum diversity gain. While V-BLAST's receiver is more complex, both are practical in the sense that receiver design and implementation is feasible.

Space-time trellis codes (STTCs) were proposed shortly afterwards; however, most research has focused on space-time block codes (STBCs), first introduced in (Tarokh et al., 1999). The idea is to extend the Alamouti scheme to systems with larger numbers of antennas (and to systems where  $n_T \neq n_R$ ); maximum likelihood (ML) decoding is feasible because the code matrices have a particular, orthogonal structure. It was soon found, however, that this approach is incapable of producing high-rate, high-diversity codes see (Gesbert et al., 2003) and (Paulraj et al., 2004) for good overviews of the development of space-time codes).

Broadly speaking, it could be said that from this point, research into code design followed two different routes, one based on algebraic construction of optimal codes, and the other based on a more practical search for possibly sub-optimal, but still useful codes.

### 2.2 Algebraic design of space-time codes

Algebraic methods have been used to design codes since the very earliest stages of the development of information theory. It is small surprise, then, that these methods have been extended to the design of space-time codes. In particular, cyclic division algebras are very useful to derive families of space-time codes with full diversity and high rate. In particular, the design objective is to find codes that achieve the diversity-multiplexing tradeoff and have maximum data rate. The constellation shape (a lattice) is included in code design, and decoding is reformulated as lattice decoding (Oggier et al., 2007). One of the main results of this work has been the definition of Perfect space-time codes; these codes are the best possible square block codes, and satisfy these criteria: full diversity, maximum coding gain, optimum diversity-multiplexing trade-off, optimum constellation shape, and uniform average energy emitted per antenna. In a very important result (Berhuy & Oggier, 2009), it was shown that Perfect codes exist only for MIMO systems with six or less antennas.

### 2.3 A simplified approach

In contrast with the theoretical, rigorous development of algebraic codes, hybrid codes are developed in a more ad hoc manner. The objective is the design of codes offering a good tradeoff between multiplexing and diversity gains; however, the design consists of a

straightforward mixture of pure diversity and pure multiplexing codes. A hybrid space-time encoder distributes the modulated data symbols among a spatial-multiplexing encoder and possibly several full-diversity encoders, as shown in Figure 3.

Fig. 3. A general hybrid space-time encoder.

In this general scheme, different space-time codes are simply stacked together and transmitted simultaneously. Conceptually, the transmitted data is divided into several layers; one spatial layer for each V-BLAST antenna, and  $N_A$  coded layers, one for each diversity encoder. Hybrid code design consists mainly in the selection of number of transmit and receive antennas, and in choosing appropriate encoders. In order for a hybrid code to be practical, a decoding algorithm must be devised that is able to take advantage of the hybrid code properties and that has low complexity. Hybrid codes are explored in more detail in the following section.

### 3. Hybrid Space-Time Codes

A large variety of hybrid space-time codes have been proposed in recent years. They differ mainly in the selection of coding layers and in decoding strategies. In this section, we identify and categorize some of the main results in hybrid code design.

#### 3.1 Quasi-Orthogonal Space-Time Codes

Space-time codes designed from orthogonal matrices can be linearly decoded in a very simple way. However, as mentioned before, full-diversity, full-rate orthogonal codes don't exist for more than two transmit antennas. Quasi-orthogonal codes (Jafarkhani, 2001), (Tirkkonen et al., 2000) use almost-orthogonal matrices to achieve full rate, while providing only partial diversity. As an example, ABBA codes have code matrices of the form

$$\begin{bmatrix} A & B \\ B & A \end{bmatrix}, \quad (6)$$

where matrix blocks A and B are  $2 \times 2$  Alamouti matrices and each one transmits a different pair of symbols. A generalization of ABBA to any number of antennas is presented in (Dai et al., 2007).

In quasi-orthogonal codes, some transmitted symbols interfering each other (in contrast, in pure spatial multiplexing schemes such as V-BLAST, all symbols interfere with each other). The decoding algorithm consists in a combination of ML decoding where there is no interference, combined with interference suppression (possibly iterative) where needed. Joint (ML) detection of all symbols simultaneously is also possible, but has increased complexity.

### 3.2 Double Space-Time Transmit Diversity

This scheme, known as DSTTD, uses two coded layers, where each layer is simply an Alamouti encoder. It is a variant of ABBA codes, where only the first column of the ABBA matrix is used, resulting in an increased data rate at the cost of less diversity. A generalization to  $2N \times 2N$  antennas, along with an efficient detector algorithm, was proposed in (Arar & Yongacoglu, 2006). In (Kwak et al., 2005) a theoretical analysis of DSTTD proved that, for a range of multiplexing gains, DSTTD offers a multiplexing-diversity tradeoff that is superior to both V-BLAST and quasi-orthogonal codes. Since DSTTD may be seen as a special case of quasi-orthogonal codes, the same decoding strategies are applicable.

### 3.3 Hybrid Codes with Multi-User Interference Suppression

A different decoding strategy is proposed in (Freitas et al., 2006). A number of different combinations of space-time encoders are proposed. In the receiver, each hybrid code layer is considered to be a different user in a multi-user system. Traditional multi-user access techniques are used to separate the symbols from each layer. In particular, the decoding process is divided in two steps, one for interference cancellation, and another for space-time decoding. In the interference cancellation step, a MIMO-MMSE spatial filter is used to eliminate the interference from undesired blocks. This filter is a traditional adaptive filter that is calculated minimizing a cost function. This technique is interesting since it leverages the large body of knowledge concerned with multi-user environments. As the number of layers increases, though, the interference is harder to eliminate; simulation results suggest that this scheme does not effectively extract diversity from the code and works best in high-SNR scenarios.

### 3.4 STBC-VBLAST

In (Mao & Motani, 2005) another decoding algorithm is proposed. In a sense, the V-BLAST iterative, successive interference cancellation (SIC) algorithm is extended to hybrid codes. It is shown that it is advantageous to decode the diversity layers first; each layer is decoded and then its interference is suppressed from the rest of the layers. This results in an increase in diversity, at the cost of some spectral efficiency. A similar detection technique is known as QR-Group Receiver (Zhao & Dubey, 2005). This scheme uses any number of stacked Alamouti encoders, and uses spatial filtering and successive interference cancellation to eliminate inter-block interference. It achieves a performance in between that of V-BLAST and Alamouti codes.

### 3.5 Linear Dispersion Codes

Linear dispersion codes (LDCs) (Hassibi & Hochwald, 2002) are an extremely flexible framework for designing space-time codes with arbitrary number of antennas. The time- and space-spreading of each transmitted symbol is specified in a dispersion matrix; this method of specifying the space-time code is so powerful that it describes a large collection of codes, from V-BLAST to perfect codes. The main disadvantage of this technique is that it is not always clear how to specify the dispersion matrices; in general, only unproven heuristics are provided.

An important property of LDCs is that they may be transformed into purely spatial codes, which means they may be decoded using a variety of algorithms, such as ordered SIC or ML decoding. It was recently shown (Longoria, 2007) that many hybrid space-time codes may be transformed into LDCs and subsequently into spatial codes. This result generalizes all the different decoding algorithms presented in this section. In the following section, two hybrid codes that build on this result are presented in detail.

## 4. Two Hybrid Space-Time Code Architectures

In this section, we present in some detail two hybrid space-time codes. Significant features of these codes are:

- Both mix spatial layers and diversity layers, allowing any number of each.
- The number of receiver antennas is also flexible, with just a minimum number specified.
- One of the codes uses Alamouti space-time encoders, while the other uses ABBA codes with either 3 or 4 transmitter antennas each.
- The receiver architecture is based on a code transformation to an LDC code, and subsequently to a purely spatial code.
- As will be seen, transformation of a hybrid code to a spatial code entails an increase in the size of the virtual channel matrix. We present a low-complexity decoder that avoids this problem.

Simulation results are presented for both architectures, and it is shown that their performance compares very favorably to the codes presented in section 3.

### 4.1 ZF-SQRD LDSTBC Scheme

This scheme is based on the hybrid architecture with an arrangement of Alamouti-STBC modules and V-BLAST layers. We show how to transform the hybrid system equation as a particular linear dispersion code. We denote by  $n_B$  and  $n_S$  the number of Alamouti blocks and number of V-BLAST antennas, respectively; at least  $n_R = n_S + n_B$  receive antennas are required. We refer to this architecture as ZF-SQRD LDSTBC. We will show how to arrive at a symbol by symbol (OSIC) decoder. This code meets the first constraint of the design method established in (Hassibi & Hochwald, 2003).

We exploit the matrices' structure to obtain a low-complexity receiver algorithm based on the sorted QR decomposition (Wubben et al., 2001). BER performance is further increased by allocating the same energy to each transmitted symbol, in contrast to other recent proposals where equal power is allocated to each antenna.

A simplified block diagram of the ZF-SQRD LDSTBC system, based on the scheme proposed in (Mao & Motani, 2005), is depicted in Figure 4. A single data stream is demultiplexed into  $n_L$  spatial layers, and each of them is mapped to the constellation chosen. The modulated stream feeds two different kinds of transmitters:  $n_S$  V-BLAST layers and  $n_B$  STBC encoders with  $n_A = 2$  antennas each one; therefore,  $n_T = n_S + n_A n_B$ .

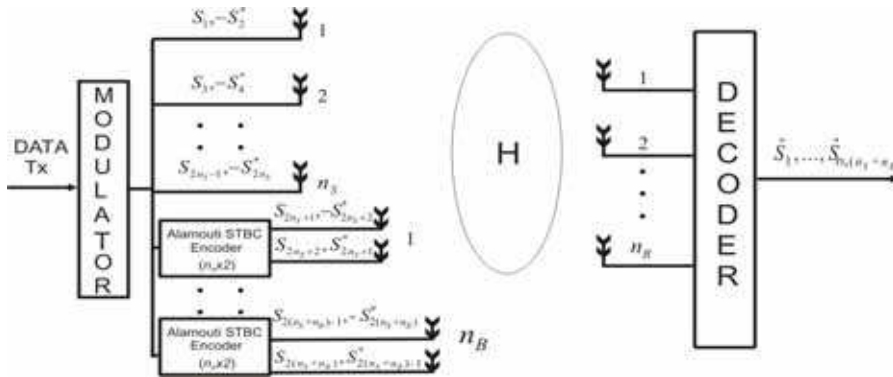


Fig. 4. ZF-SQRD LDSTBC Transmitter/Receiver Architecture

It is assumed that  $n_R \geq n_S + n_B$ . In the transmission of one block, the symbol sequence  $s_1, s_2, \dots, s_{nsym}$ , where  $nsym = n_A(n_S + n_B)$  is transmitted. The mapping of symbols to antennas is shown in Table I. The fraction of power allocated to the VBLAST layers is given by:

$$P_S = \frac{2}{n_A(n_S + n_B)}, \tag{7}$$

and the fraction allocated to the Alamouti encoder is given by

$$P_A = \frac{P_S}{n_A n_B}. \tag{8}$$

	Spatial Antennas	STBC Blocks $B=1,2,\dots,n_B$	
Time	Antenna $V=1,2,\dots,n_S$	Antenna 1	Antenna 2
$t$	$s_V$	$s_{kn_A+1}$	$s_{kn_A+2}$
$T+T$	$-s_{V+1}^*$	$-s_{kn_A+2}^*$	$s_{kn_A+1}^*$

Table 1. ZF-SQRD-LDSTBC Symbol to Antenna Mapping with  $k = B - 1 + n_S$



This allocation results in all symbols being transmitted with the same power. Under the assumption of perfect CSI at the receiver, the detection and decoding process of the transmitted signal vector  $S$ , at the  $m^{th}$  time block slice, where  $m = 1, 2$  and  $n_A = 2$ , the receive signal can be written as:

$$\begin{bmatrix} y_1^{(1)} & y_1^{(2)} \\ \vdots & \vdots \\ y_{n_R}^{(1)} & y_{n_R}^{(2)} \end{bmatrix} = \begin{bmatrix} h_{1,1} & h_{1,2} & \cdots & h_{1,n_T} \\ \vdots & \vdots & \ddots & \vdots \\ h_{n_R,1} & h_{n_R,2} & \cdots & h_{n_R,n_T} \end{bmatrix} \begin{bmatrix} S_{spa} \\ S_A \end{bmatrix} + \begin{bmatrix} n_1^{(1)} & n_1^{(2)} \\ \vdots & \vdots \\ n_{n_R}^{(1)} & n_{n_R}^{(2)} \end{bmatrix}, \tag{9}$$

or equivalently,

$$Y = HS + N. \tag{10}$$

In equation (9) and the following, the sub indices indicate the receiver antenna, and the super indices indicate the block emission time. Matrix  $Y \in C^{n_R \times 2}$  represents the symbols received in a block. Matrix  $H$  is the channel matrix defined above. Matrix  $N \in C^{n_R \times 2}$  represents the noise added to each received symbol. Matrix  $S$  is composed for two blocks: The matrix  $S_{spa}$  corresponds to the symbols transmitted by VBLAST layers and the matrix  $S_A$  to the symbols transmitted by STBC encoders. The spatial multiplexing block  $S_{spa}$  is defined as:

$$S_{spa} = \begin{bmatrix} s_1 & -s_2^* \\ s_3 & -s_4^* \\ \vdots & \vdots \\ s_{2n_S-1} & -s_{2n_S}^* \end{bmatrix} = \begin{bmatrix} s_1^{(1)} & s_1^{(2)} \\ s_2^{(1)} & s_2^{(2)} \\ \vdots & \vdots \\ s_{n_S}^{(1)} & s_{n_S}^{(2)} \end{bmatrix}, \tag{11}$$

and the STBC block is defined as:

$$S_A = \begin{bmatrix} S_1^A \\ \vdots \\ S_{n_B}^A \end{bmatrix} = \begin{bmatrix} S_1^{(1)A} & S_1^{(2)A} \\ \vdots & \vdots \\ S_{n_B}^{(1)A} & S_{n_B}^{(2)A} \end{bmatrix}, \tag{12}$$

where each element of equation (4) is given by:

$$\begin{bmatrix} S_B^{(1)A} & S_B^{(2)A} \end{bmatrix} = \begin{bmatrix} S_{kn_A+1} & -S_{kn_A+2}^* \\ S_{kn_A+2} & S_{kn_A+1}^* \end{bmatrix}, \tag{13}$$

with  $B = 1, 2, \dots, n_B$  and  $k = B - 1 + n_S$ . In equations (11) and (12), the matrix on the left is a direct mapping from Table 1; the notation of the matrix on the right, where antenna number and symbol period are made explicit, is adopted to simplify the explanation of the receiver algorithm. Reformulating the system equation (9) as a linear dispersion code (Longoria et al., 2007), we have:

$$\left[ y_1^{(1)} \ y_1^{(2)*} \ \dots \ y_{n_R}^{(1)} \ y_{n_R}^{(2)*} \right]^T = \left[ H_{spa} \ H_A \right] S_{LD} + \left[ n_1^{(1)} \ n_1^{(2)*} \ \dots \ n_{n_R}^{(1)} \ n_{n_R}^{(2)*} \right]^T. \quad (14)$$

Equation (14) can be expressed in compact form as:

$$Y_{LD} = H_{LD} S_{LD} + N_{LD}, \quad (15)$$

where  $H_{LD}$  is composed of two blocks is named Linear Dispersion Matrix, one corresponding to the V-BLAST layers and another to the STBC layers. The V-BLAST block  $H_{spa}$  is given by:

$$H_{spa} = \begin{bmatrix} H_{1,1}^{spa} & H_{1,2}^{spa} & \dots & H_{1,n_S}^{spa} \\ \vdots & \vdots & \ddots & \vdots \\ H_{n_R,1}^{spa} & H_{n_R,2}^{spa} & & H_{n_R,n_S}^{spa} \end{bmatrix}, \quad (16)$$

where

$$H_{i,j}^{spa} = \begin{bmatrix} h_{i,j} & 0 \\ 0 & -h_{i,j}^* \end{bmatrix}, \quad (17)$$

for  $i = 1, 2, \dots, n_R$  and  $j = 1, 2, \dots, n_S$ . The STBC block  $H_A$  is itself a block matrix; it is given by:

$$H_A = \begin{bmatrix} H_{1,1}^A & H_{1,2}^A & \dots & H_{1,n_S}^A \\ \vdots & \vdots & \ddots & \vdots \\ H_{n_R,1}^A & H_{n_R,2}^A & & H_{n_R,n_S}^A \end{bmatrix}, \quad (18)$$

where each element of equation (18) is given by:

$$H_{k,B}^A = \begin{bmatrix} h_{k,n_A B + n_S - 1} & h_{k,n_A B + n_S} \\ h_{k,n_A B + n_S}^* & h_{k,n_A B + n_S - 1}^* \end{bmatrix}, \quad (19)$$

for  $k = 1, 2, \dots, n_R$  and  $B = 1, 2, \dots, n_B$ . The matrix  $H_{i,j}^{spa}$  links the  $j^{th}$  spatial antenna with the  $i^{th}$  receiver antenna. Likewise,  $H_{k,B}^A$  links the  $B^{th}$  STBC block to the  $k^{th}$  receiver antenna. To complete the reformulation of system equation (9), it remains to rearrange matrix  $S$ . We define  $S_{LD}$  as:

$$S_{LD} = \begin{bmatrix} S_{LD}^{spa} \\ S_{LD}^A \end{bmatrix} \tag{20}$$

where

$$S_{LD}^{spa} = [s_1^{(1)} \ s_1^{(2)} \ \dots \ s_{n_s}^{(1)} \ s_{n_s}^{(2)}]^T \tag{21}$$

and

$$S_{LD}^A = [S_1^{(1)A} \ S_2^{(1)A} \ \dots \ S_{n_B}^{(1)A}]^T. \tag{22}$$

The reformulation of equation (9) as equation (14) transforms the hybrid code to a simpler, equivalent purely spatial system with  $N_T = n_A(n_s + n_b)$  transmit antennas and without distinction between the STBC and VBLAST layers. This simpler system is shown in Figure 5.

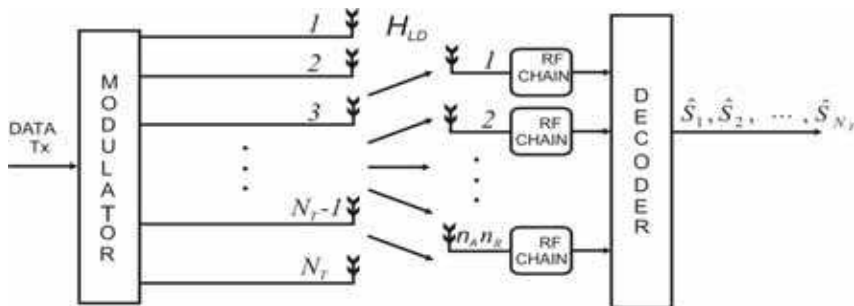


Fig. 5. ZF-SQRD LDSTBC Architecture Transmitter/Receiver as Linear Dispersion Code

#### 4.2 ZF-SQRD LQOSTBC Scheme

The hybrid code called ZF-QR-SIC-LQOSTBC (Cortez et al., 2008) allows the use of any number of V-BLAST antennas, and any number of ABBA encoders of 3 or 4 antennas each. A block diagram of the ZF-SQRD LQOSTBC is shown in Figure 6.

Of the  $n_T$  transmit antennas,  $n_s$  are spatially multiplexed. There are  $n_B$  ABBA encoders, of  $n_A \in \{3, 4\}$  antennas each, so that  $n_T = n_s + n_B \cdot n_A$ . It is assumed that  $n_R \geq n_s + n_B$ . We will assume  $n_A = 4$ ; it is straightforward to extend the results to the case  $n_A = 3$ . In the transmission of one block, the symbol sequence  $\{s_i\}_{i=1}^{4(n_s + n_B)}$  is transmitted. The mapping of

symbols to antennas is shown in Table 2. Using this code,  $n_s + n_B$  symbols are transmitted per channel use, for a code rate equal to

$$\frac{n_s + n_B}{n_T} \tag{23}$$

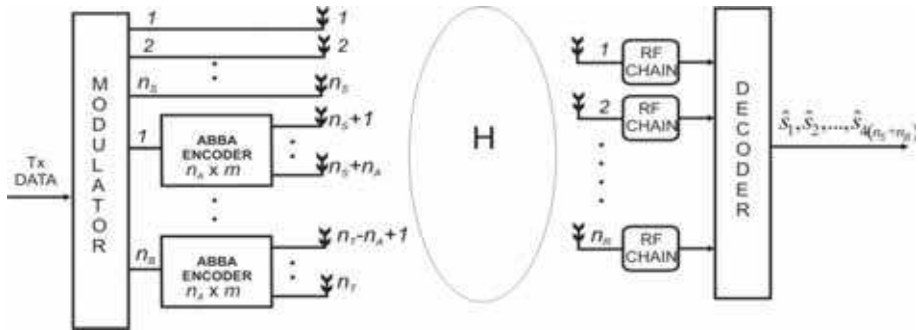


Fig. 6. ZF-SQRD LQOSTBC Architecture Transmitter/Receiver

ANTENNA	Symbol Period			
	1	2	3	4
(VBLAST)				
1	$s_1$	$-s_2^*$	$s_3$	$-s_4^*$
2	$s_5$	$-s_6^*$	$s_7$	$-s_8^*$
$\vdots$	$\vdots$	$\vdots$	$\vdots$	$\vdots$
$n_s$	$s_{k-3}$	$-s_{k-2}^*$	$s_{k-1}$	$-s_k^*$
(ABBA)				
$n_s + 1$	$s_{k+1}$	$-s_{k+2}^*$	$s_{k+3}$	$-s_{k+4}^*$
$n_s + 2$	$s_{k+2}$	$s_{k+1}^*$	$s_{k+4}$	$s_{k+3}^*$
$\vdots$	$\vdots$	$\vdots$	$\vdots$	$\vdots$
$n_T$	$s_{k+4n_B}$	$s_{k+4n_B-1}^*$	$s_{k+4n_B-2}$	$s_{k+4n_B-3}^*$

Table 2. ZF-SQRD LQOSTBC Symbol to Antenna Mapping with  $k = 4n_s$

Since the transmitter has no knowledge of the channel, all symbols must be transmitted with equal energy. In the ABBA layers, each symbol’s transmission is spread across multiple time intervals; in consequence, the signal constellations must be scaled accordingly. If  $E_v$  is the average energy of the signal constellation employed by each antenna in the VBLAST layers, then the average constellation energy  $E_a$  of the ABBA layers is given by  $E_a = E_v/n_a$ . It should be noted that the coding schemes referenced above use a single constellation, resulting in unequal symbol energy and suboptimal BER performance.

The system equation for ZF-SQRD LQOSTBC over four symbol periods may be written as follows, where subindices indicate antenna number, and superindices indicate symbol period within a block:

$$\begin{bmatrix} y_1^{(1)} \cdots y_1^{(4)} \\ \vdots \quad \ddots \quad \vdots \\ y_{n_R}^{(1)} \cdots y_{n_R}^{(4)} \end{bmatrix} = \begin{bmatrix} h_{1,1} & h_{1,2} & \cdots & h_{1,n_T} \\ \vdots & \vdots & \ddots & \vdots \\ h_{n_R,1} & h_{n_R,2} & \cdots & h_{n_R,n_T} \end{bmatrix} \begin{bmatrix} S_{abba} \\ S_A \end{bmatrix} + \begin{bmatrix} n_1^{(1)} \cdots n_1^{(4)} \\ \vdots \quad \ddots \quad \vdots \\ n_{n_R}^{(1)} \cdots n_{n_R}^{(4)} \end{bmatrix}, \tag{24}$$

or equivalently,

$$Y = HS + N. \tag{25}$$

Matrix  $Y \in C^{n_R \times 4}$  represents the symbols received in a block. Matrix  $H$  is the channel matrix defined above. Matrix  $N \in C^{n_R \times 4}$  represents the noise added to each received symbol. Matrix  $S$  is composed of a spatial multiplexing block and  $n_B$  ABBA blocks. The spatial multiplexing block  $S_{spa}$  is defined as:

$$S_{spa} = \begin{bmatrix} s_1 & -s_2^* & s_3 & -s_4^* \\ \vdots & \vdots & \vdots & \vdots \\ s_{4n_S-3} & -s_{4n_S-2}^* & s_{4n_S-1} & -s_{4n_S}^* \end{bmatrix} = \begin{bmatrix} s_1^{(1)} \cdots s_1^{(4)} \\ \vdots \quad \vdots \\ s_{n_S}^{(1)} \cdots s_{n_S}^{(4)} \end{bmatrix}, \tag{26}$$

which corresponds to the VBLAST layer mapping in Table 2. The ABBA block is defined as:

$$S_{abba} = [S_1^{abba} \ S_2^{abba} \ \cdots \ S_{n_B}^{abba}], \tag{27}$$

where every element of equation (27) is given by:

$$S_B^{abba} = \begin{bmatrix} s_{k+1} & -s_{k+2}^* & s_{k+3} & -s_{k+4}^* \\ s_{k+2} & s_{k+1}^* & s_{k+4} & s_{k+3}^* \\ s_{k+3} & -s_{k+4}^* & s_{k+1} & -s_{k+2}^* \\ s_{k+4} & s_{k+3}^* & s_{k+2} & s_{k+1}^* \end{bmatrix} = \begin{bmatrix} s_{l-3}^{(1)} \cdots s_{l-3}^{(4)} \\ s_{l-2}^{(1)} \cdots s_{l-2}^{(4)} \\ s_{l-1}^{(1)} \cdots s_{l-1}^{(4)} \\ s_l^{(1)} \cdots s_l^{(4)} \end{bmatrix}, \tag{28}$$

with  $l = n_S + 4B$ ,  $k = 4(B - 1 + n_S)$  and  $B = 1, 2, \dots, n_B$ . Rewriting the system equation (24) as a linear dispersion code, we have:

$$\begin{bmatrix} y_1^{(1)} \\ y_1^{(2)*} \\ y_1^{(3)} \\ y_1^{(4)*} \\ \vdots \\ y_{n_R}^{(1)} \\ y_{n_R}^{(2)*} \\ y_{n_R}^{(3)} \\ y_{n_R}^{(4)*} \end{bmatrix} = [H_{spa} \ H_{abba}] S_{LD} + \begin{bmatrix} n_1^{(1)} \\ n_1^{(2)*} \\ n_1^{(3)} \\ n_1^{(4)*} \\ \vdots \\ n_{n_R}^{(1)} \\ n_{n_R}^{(2)*} \\ n_{n_R}^{(3)} \\ n_{n_R}^{(4)*} \end{bmatrix}, \quad (29)$$

expressed in compact form as:

$$Y_{LD} = H_{LD} S_{LD} + N_{LD}, \quad (30)$$

where  $H_{LD}$  is a linear dispersion matrix with two blocks, one corresponding to the V-BLAST layers and another to the ABBA layers. The V-BLAST block  $H_{spa}$  is given by:

$$H_{spa} = \begin{bmatrix} H_{1,1}^{spa} & H_{1,2}^{spa} & \cdots & H_{1,n_S}^{spa} \\ \vdots & \vdots & \ddots & \vdots \\ H_{n_R,1}^{spa} & H_{n_R,2}^{spa} & & H_{n_R,n_S}^{spa} \end{bmatrix}, \quad (31)$$

where

$$H_{i,j}^{spa} = \begin{bmatrix} h_{i,j} & 0 & 0 & 0 \\ 0 & -h_{i,j}^* & 0 & 0 \\ 0 & 0 & h_{i,j} & 0 \\ 0 & 0 & 0 & -h_{i,j}^* \end{bmatrix}, \quad (32)$$

for  $i = 1, 2, \dots, n_R$  and  $j = 1, 2, \dots, n_S$ . The ABBA block  $H_{abba}$  is itself a block matrix; it is given by:

$$H_{abba} = \begin{bmatrix} H_{1,1}^{abba} & H_{1,2}^{abba} & \cdots & H_{1,n_S}^{abba} \\ \vdots & \vdots & \ddots & \vdots \\ H_{n_R,1}^{abba} & H_{n_R,2}^{abba} & \cdots & H_{n_R,n_S}^{abba} \end{bmatrix}, \tag{33}$$

where every element of equation (33) is given by:

$$H_{i,k}^{abba} = \begin{bmatrix} h_{i,l-3} & h_{i,l-2} & h_{i,l-1} & h_{i,l} \\ h_{i,l-2}^* & -h_{i,l-3}^* & h_{i,l}^* & -h_{i,l-1}^* \\ h_{i,l-1} & h_{i,l} & h_{i,l-3} & h_{i,l-2} \\ h_{i,l}^* & -h_{i,l-1}^* & h_{i,l-2}^* & -h_{i,l-3}^* \end{bmatrix}, \tag{34}$$

for  $i = 1, 2, \dots, n_R$ ,  $k = 1, 2, \dots, n_B$  and  $l = n_S + 4B$ . The matrix  $H_{i,j}^{spa}$  of  $H_{LD}$  that links the  $j^{th}$  spatial antenna with the  $i^{th}$  receiver antenna. Likewise,  $H_{i,k}^{abba}$  links the  $k^{th}$  ABBA block to the  $i^{th}$  receiver antenna. To complete the reformulation of system equation (24), it remains to rearrange matrix  $S$ . We define  $S_{LD}$  as:

$$S_{LD} = \begin{bmatrix} S_{LD}^{spa} & S_{LD}^{abba} \end{bmatrix}^T \tag{35}$$

where

$$S_{LD}^{spa} = \begin{bmatrix} s_1^{(1)} & s_1^{(2)} & s_1^{(3)} & s_1^{(4)} & \cdots & s_{n_S}^{(1)} & s_{n_S}^{(2)} & s_{n_S}^{(3)} & s_{n_S}^{(4)} \end{bmatrix}^T \tag{36}$$

and the ABBA block for  $n_A = 4$  is, then, given by:

$$S_{LD}^{abba} = \begin{bmatrix} s_{n_S+1}^{(1)} & s_{n_S+2}^{(1)} & s_{n_S+3}^{(1)} & s_{n_S+4}^{(1)} & \cdots & s_{l-3}^{(1)} & s_{l-2}^{(1)} & s_{l-1}^{(1)} & s_l^{(1)} \end{bmatrix}^T. \tag{37}$$

We have rewritten the hybrid space-time matrices as linear dispersion code matrices. Now we can substitute the original V-BLAST plus ABBA hybrid transceiver with a simpler, purely spatial system with  $N_T = 4n_S + n_A n_B$  transmit antennas like is depicted in Figure 7 and without distinction between the ABBA and VBLAST layers.

### 5. Receiver Architectures for Hybrid Space-Time Codes

Since schemes ZF-SQRD LSTBC and ZF-SQRD LQOSTBC are equivalent to a purely spatial system with  $N_T$  transmit antennas, it is possible to propose a linear detector based on the

sorted QR decomposition and OSIC, that takes advantage of the structure of the linear dispersion matrices to achieve low complexity and high performance.

### 5.1 OSIC Detection for Hybrid Schemes Proposed

We first calculate *HC Sorted QR* (Hybrid Coding Sorted QR) of the matrix  $H_{LD} = Q_{LD}R_{LD}$  where  $Q_{LD}$  is a unitary matrix and  $R_{LD}$  is an upper triangular matrix. By multiplying the received signal equations (10) and (35) by  $Q_{LD}^H$ , the modified received vector is:

$$\tilde{Y}_{LD} = Q_{LD}^H Y_{LD} = R_{LD} S_{LD} + \tilde{N}_{LD}, \quad (38)$$

if vector  $S_{LD}$  is transmitted. Note that the statistical properties of the noise term  $\tilde{N}_{LD}$  remain unchanged. Due to the upper triangular structure of  $R_{LD}$ , the  $k^{\text{th}}$  element of  $\tilde{Y}_{LD}$  is:

$$\tilde{y}_k = r_{k,k} s_k + \sum_{i=k+1}^{N_T} r_{k,i} s_i + \tilde{n}_k. \quad (39)$$

Symbols are estimated in sequence, from lower stream to higher stream, using OSIC; assuming that all previous decisions are correct; the interference can be perfectly cancelled in each step except for the additive noise. The estimated symbol  $s_k$  is given by:

$$s_k = \mathbf{D} \left[ \frac{y_k - \sum_{i=k+1}^{N_T} r_{k,i} \hat{s}_i}{r_{k,k}} \right], \quad (40)$$

where  $\hat{s}_k$  is the estimate of  $s_k$  and  $\mathbf{D}[\cdot]$  is a decision device that maps its argument to the closest constellation point. Therefore the receiver requires calculating the QR decomposition for the linear dispersion matrix  $H_{LD}$ ; the main challenge lies in finding the most efficient way to obtain this decomposition.

We use the permutation vector order provided by *HC Sorted QR* algorithm to reorder the received symbols; the QR decomposition is obtained using the modified Gram-Schmidt (MGS) algorithm.

### 5.2 HC Sorted QR Decomposition

Matrix  $H_{LD}$  is  $N_T \times n_A n_R$  for both hybrid schemes. A direct application of MGS on it would result in unacceptable complexity. However, taking advantage of the structure imposed on  $H_{LD}$  by the proposed code, we can decrease this complexity significantly. We now explain how this simplification is obtained.

From the equations (15) and (30) we can see that the structure presented for the  $H_{LD}$  matrix allows us to reduce the computational complexity that is required for to calculate the *HC*



Sorted QR decomposition, since many of the elements of each matrix are equal, and their locations in each matrix are fixed and can be calculated in advance. This method involves obtaining the QR decomposition of the  $H_{LD}$  matrix in two stages: first we obtain the QR decomposition corresponding to the spatial layers of the hybrid system; in the second stage we calculate the QR decomposition for the diversity layers.

As a first step, we calculate the QR decomposition  $H = Q_m R_m$  using the Sorted QR algorithm; in this process, we also produce vector *order* which specifies the detection order of the spatial layers. Then, using  $Q_m$  and  $R_m$ , and non normalized columns of the matrix H, we build the matrices  $H_{div}^{ala}$  or  $H_{div}^{abba}$ . The next step is analogous to MGS: column  $k + 1$  is normalized and used to fill column  $k+2$  of each block (Alamouti/ABBA); the process is repeated for the remaining columns for each block of  $H_{div}^{ala}$  or  $H_{div}^{abba}$ . In the process, matrix  $R_{LD}$  is also calculated. A block diagram of the process is shown in the Figure 7.

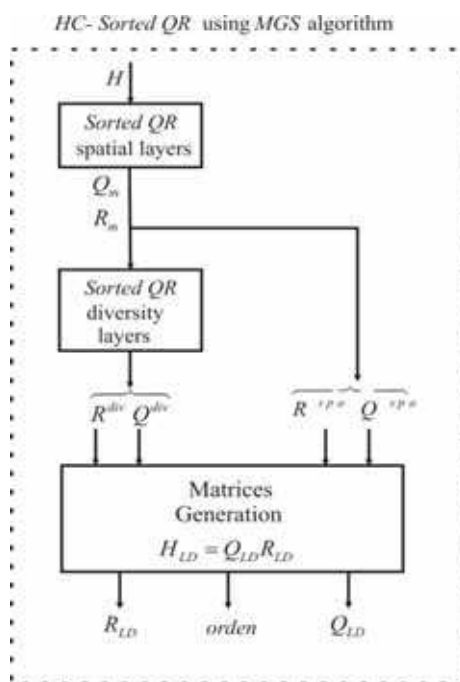


Fig. 7. HC Sorted QR Process Using MGS Algorithm

The structure of matrices  $Q_{LD}$  and  $R_{LD}$ , and their relation to  $Q_m$  and  $R_m$ , has been detailed in (Cortez et al., 2007), (Kim et al., 2006), (Le et al., 2005). The complete process is presented in two stages. In the first stage the algorithm 1 takes the channel matrix  $H$  and outputs the intermediate matrices  $Q_m$ ,  $R_m$  and vector *order*.

---

**Algorithm 1. HC Sorted QR of the Spatial Layers**


---

```

1: INPUT:  $H^{n_R \times n_T}$ ,  $L$ ,  $nsym$ ,  $n_S$ 
2: OUPUT:  $Q_m$ ,  $R_m$ ,  $order$ 
3:  $Q_m = H$ ,  $R_m^{n_T \times n_T} = 0$ ,  $orden = [1 : 1 : nsym]$ 
4: for  $i = 1$  to  $n_S$  do
5:    $k = \arg \min_{j=i:n_S} \|Q_m(:, j)\|$ 
6:   Exchange columns  $i$  and  $k$  of  $Q_m$  and  $R_m$ 
7:   Exchange columns  $Li : -1 : i(L - 1) + 1$  and  $Lk : -1 : k(L - 1) + 1$  of  $order$ 
8:    $R_m(i, i) = \|Q_m(:, i)\|_2$ 
9:    $Q_m(:, i) = Q_m(:, i) / R_m(i, i)$ 
10:  for  $j = i + 1$  to  $n_T$  do
11:     $R_m(i, j) = Q_m(:, i)^H Q_m(:, j)$ 
12:     $Q_m(:, j) = Q_m(:, j) - Q_m(:, i)R_m(i, j)$ 
13:  endfor
14: endfor

```

The structure for the matrices  $Q_m$  and  $R_m$  are:

$$Q_m = \begin{bmatrix} q_{1,1} & \cdots & q_{1,n_S} & \underline{h}_{1,n_S+1} & \cdots & \underline{h}_{1,n_T} \\ q_{2,1} & \cdots & q_{2,n_S} & \underline{h}_{2,n_S+1} & \cdots & \underline{h}_{2,n_T} \\ \vdots & & \vdots & \vdots & \ddots & \vdots \\ q_{n_R,1} & \cdots & q_{n_R,n_S} & \underline{h}_{n_R,n_S+1} & \cdots & \underline{h}_{n_R,n_T} \end{bmatrix}, \quad (41)$$

$$R_m = \begin{bmatrix} r_{1,1} & \cdots & r_{1,n_S} & r_{1,n_S+1} & \cdots & r_{1,n_T} \\ 0 & \cdots & r_{2,n_S} & r_{2,n_S+1} & \cdots & r_{2,n_T} \\ \vdots & & \vdots & \vdots & \ddots & \vdots \\ 0 & 0 & \cdots & r_{n_S,n_S} & \cdots & r_{n_S,n_T} \end{bmatrix}. \quad (42)$$

We choose the first  $n_S$  columns of  $Q_m$  and the first  $n_S$  rows of  $R_m$  to built the matrices  $Q^{spa}$  and  $R^{spa}$  with the next structure:

$$Q^{spa} = \begin{bmatrix} q_{1,1} & q_{1,2} & \cdots & q_{1,n_S} \\ q_{2,1} & q_{2,2} & \cdots & q_{2,n_S} \\ \vdots & \vdots & & \vdots \\ q_{n_R,1} & q_{n_R,2} & \cdots & q_{n_R,n_S} \end{bmatrix}, \tag{43}$$

$$R^{spa} = \begin{bmatrix} r_{1,1} & \cdots & r_{1,n_S} & r_{1,n_S+1} & \cdots & r_{1,n_T} \\ 0 & \cdots & r_{2,n_S} & r_{2,n_S+1} & \cdots & r_{2,n_T} \\ \vdots & & \ddots & \vdots & \ddots & \vdots \\ 0 & & 0 & \cdots & r_{n_S,n_S} & \cdots & r_{n_S,n_T} \end{bmatrix}. \tag{44}$$

The matrices  $Q^{spa}$  and  $R^{spa}$  represent the contribution of the spatial layers in both hybrid schemes. The columns with elements  $\underline{h}_{i,j}$  in equation (41) are non normalized columns that we used to build the matrices  $H_{div}^{ala}$  and  $H_{div}^{abba}$  that are required in the second stage of the QR decomposition for the diversity layers. In the case of ZF-SQRD LDSTBC the matrix  $H_{div}^{ala}$  has the following structure:

$$H_{div}^{ala} = \begin{bmatrix} \underline{h}_{1,n_S+1} & \underline{h}_{1,n_S+2} & \cdots & \underline{h}_{1,n_T-1} & \underline{h}_{1,n_T} \\ \underline{h}_{1,n_S+2}^* & -\underline{h}_{1,n_S+1}^* & \cdots & \underline{h}_{1,n_T}^* & -\underline{h}_{1,n_T-1}^* \\ \vdots & \vdots & & \vdots & \vdots \\ \underline{h}_{n_R,n_S+2}^* & -\underline{h}_{n_R,n_S+1}^* & \cdots & \underline{h}_{n_R,n_T}^* & -\underline{h}_{n_R,n_T-1}^* \end{bmatrix}. \tag{45}$$

For the case of ZF-SQRD LQOSTBC the matrix  $H_{div}^{abba}$  with  $n_A = 4$  has the structure:

$$H_{div}^{abba} = \begin{bmatrix} \underline{h}_{1,n_S+1} & \underline{h}_{1,n_S+3} & \cdots & \underline{h}_{1,n_T-3} & \underline{h}_{1,n_T-1} \\ \underline{h}_{1,n_S+2}^* & \underline{h}_{1,n_S+4}^* & \cdots & \underline{h}_{1,n_T-2}^* & \underline{h}_{1,n_T}^* \\ \vdots & \vdots & & \vdots & \vdots \\ \underline{h}_{n_R,n_S+4}^* & \underline{h}_{n_R,n_S+2}^* & \cdots & \underline{h}_{n_R,n_T}^* & \underline{h}_{n_R,n_T-2}^* \end{bmatrix}. \tag{46}$$

Once the matrix  $H_{div}^{ala/abba}$  is found, the next step is to apply the Sorted QR decomposition on it. This calculation may be carried out using Algorithm 2 below; the ordering among elements of the matrix  $H_{div}^{ala/abba}$  is by block and not by column. It is only necessary to

calculate the odd rows and columns of matrices  $Q^{div}$  and  $R^{div}$ . It can be seen as  $H_{div}^{ala}$  and  $H_{div}^{abba}$  have the same structure, the matrix  $H_{div}^{abba}$  can be seen as a particular case of  $H_{div}^{ala}$  with two Alamouti coders in each block ABBA. The above consideration allows us to use the same algorithm to calculate the *HC Sorted QR* decomposition for both schemes. The matrices  $Q^{div}$  and  $R^{div}$  generated in this part of the process represent the contribution of diversity layers in the *HC Sorted QR* decomposition.

---

Algorithm 2. *HC Sorted QR* of the Diversity Layers

---

```

1: INPUT:  $H_{div}^{ala/abba}$ ,  $L$ ,  $nsym$ ,  $n_B$ ,  $n_S$ ,  $order$ 
2: OUPUT:  $Q^{div}$ ,  $R^{div}$ ,  $order$ 
3:  $Q^{div} = H_{div}^{ala/abba}$ ,  $R^{div} = 0$ ,  $m = Ln_S$ 
4: for  $i = 1 : 2$  to  $2n_B$  do
5:    $k = \arg \min_{j=i:2:2n_B} \|Q^{div}(:,j)\|$ 
6:   Exchange columns  $i$  and  $i+1$  for  $k$  and  $k+1$  of  $Q^{div}$  and  $R^{div}$ 
7:   Exchange columns  $m + Li : -1 : m + i(L - 1) + 1$  and
      $m + Lk : -1 : m + k(L - 1) + 1$  of  $order$ 
8:    $R^{div}(i,i) = \|Q^{div}(:,i)\|_2$ 
9:    $Q^{div}(:,i) = Q^{div}(:,i) / R^{div}(i,i)$ 
10:   $R^{div}(i+1,i+1) = -R^{div}(i,i)$ 
11:   $Q^{div}(1:2:Ln_R-1,i+1) = -Q^{div}(2:2:Ln_R,i)^*$ 
12:   $Q^{div}(2:2:Ln_R,i+1) = Q^{div}(1:2:Ln_R-1,i)^*$ 
13:  for  $j = i+1$  to  $2n_B$  do
14:     $R^{div}(i,j) = Q^{div}(:,i)^H Q^{div}(:,j)$ 
15:  endfor
16:   $R^{div}(i+1,i+2:2:Ln_B-1) = R^{div}(i,i+3:2:Ln_B)^*$ 
17:   $R^{div}(i+1,i+3:2:Ln_B) = -R^{div}(i,i+2:2:Ln_B-1)^*$ 
18:  for  $j = i+1$  to  $2n_B$  do
19:     $Q^{div}(:,j) = Q^{div}(:,j) - Q^{div}(:,i)R^{div}(i,j)$ 
20:     $Q^{div}(:,j) = Q^{div}(:,j) - Q^{div}(:,i+1)R^{div}(i+1,j)$ 
21:  endfor
22: endfor

```

The matrices  $Q_{LD}$  and  $R_{LD}$  are generated from the matrices  $Q^{spa}$ ,  $R^{spa}$ ,  $Q^{div}$  and  $R^{div}$ . The construction process is described in Algorithms 3 and 4. Once the matrices  $Q_{LD}$  and  $R_{LD}$  are generated the detection of the received symbols was carried out according to the procedure described in section 5.1.

---

Algorithm 3. Generation of matrices  $Q_{LD}$  and  $R_{LD}$  for the scheme ZF-SQRD LDSTBC

---

```

1: INPUT:  $Q^{spa}$ ,  $R^{spa}$ ,  $Q^{div}$ ,  $R^{div}$ ,  $n_B$ ,  $n_S$ 
2: OUPUT:  $Q_{LD}$ ,  $R_{LD}$ 
3:  $col = 1$ 
4: for  $i = 1$  to  $n_S$  do
5:    $Q_{LD}^{spa}(1:2:2n_R - 1, col) = Q^{spa}(:, k)$ 
6:    $col = col + 1$ 
7:    $Q_{LD}^{spa}(2:2:2n_R, col) = -Q^{spa}(:, k)^*$ 
8:    $col = col + 1$ 
9: endfor
10:  $row = 1$ 
11: for  $i = 1$  to  $n_S$  do
12:    $R_{LD}^{spa}(row, 1:2:2n_S - 1) = R^{spa}(k, 1:n_S)$ 
13:    $R_{LD}^{spa}(row, 1:2:2n_S - 1) = R^{spa}(k, 1:n_S)$ 
14:    $row = row + 2$ 
15: endfor
16:  $row = 1, col = 2n_S + 1$ 
17: for  $i = 1$  to  $n_S + n_B$  do
18:   for  $j = 1$  to  $n_B$  do
19:      $R_{LD}^{spa}(row, col) = R^{spa}(i, 2j - 1 + n_S)$ 
20:      $R_{LD}^{spa}(row, col + 1) = R^{spa}(i, 2j + n_S)$ 
21:      $R_{LD}^{spa}(row + 1, col) = R^{spa}(i, 2j + n_S)^*$ 
22:      $R_{LD}^{spa}(row + 1, col + 1) = -R^{spa}(i, 2j - 1 + n_S)^*$ 
23:      $col = col + 2$ 
24:   endfor
25:    $col = 2n_S + 1$ 
26:    $row = row + 2$ 
27: endfor

```

$$28: R_{LD}^{ala}(2n_S + 1 : 2(n_S + n_B), 2n_S + 1 : 2(n_S + n_B)) = R^{div}$$

$$29: R_{LD} = \begin{bmatrix} R_{LD}^{spa} \\ R_{LD}^{ala} \end{bmatrix}, Q_{LD} = \begin{bmatrix} Q_{LD}^{spa} & Q^{div} \end{bmatrix}$$

---

Algorithm 4. Generation of matrices  $Q_{LD}$  and  $R_{LD}$  for the scheme ZF-SQRD LQOSTBC

---

```

1: INPUT:  $Q^{spa}$ ,  $R^{spa}$ ,  $Q^{div}$ ,  $R^{div}$ ,  $n_B$ ,  $n_S$ 
2: OUPUT:  $Q_{LD}$ ,  $R_{LD}$ 
3:  $row = 1$ ;  $k = 4n_S$ 
4: for  $i = 1$  to  $n_S$  do
5:    $R_{LD}^{spa}(row, 1 : 4 : k) = R^{spa}(i, 1 : n_S)$ 
6:    $R_{LD}^{spa}(row + 1, 2 : 4 : k) = -R^{spa}(i, 1 : n_S)^*$ 
7:    $R_{LD}^{spa}(row + 2, 3 : 4 : k) = R^{spa}(i, 1 : n_S)$ 
8:    $R_{LD}^{spa}(row + 3, 4 : 4 : k) = -R^{spa}(i, 1 : n_S)^*$ 
9:    $row = row + 4$ 
10: endfor
11:  $col = 1$ 
12: for  $i = 1$  to  $n_S$  do
13:    $Q_{LD}^{spa}(1 : 4 : 4n_R, col) = Q^{spa}(:, i)$ 
14:    $Q_{LD}^{spa}(2 : 4 : 4n_R, col + 1) = Q^{spa}(:, i)^*$ 
15:    $Q_{LD}^{spa}(3 : 4 : 4n_R, col + 2) = Q^{spa}(:, i)$ 
16:    $Q_{LD}^{spa}(4 : 4 : 4n_R, col + 3) = Q^{spa}(:, i)^*$ 
17:    $col = col + 4$ 
18: endfor
19:  $row = 1, col = 4n_S + 1, col2 = n_S + 1$ 
20: for  $i = 1$  to  $n_S$  do
21:   for  $j = 1$  to  $n_B$  do
22:      $R_{LD}^{abba}(row, col) = R^{spa}(i, col2)$ 
23:      $R_{LD}^{abba}(row + 1, col) = R^{spa}(i, col2 + 1)^*$ 
24:      $R_{LD}^{abba}(row + 2, col) = R^{spa}(i, col2 + 2)$ 
25:      $R_{LD}^{abba}(row + 3, col) = R^{spa}(i, col2 + 3)^*$ 

```

```

26:    $R_{LD}^{abba}(row, col + 2) = R^{spa}(i, col2)$ 
27:    $R_{LD}^{abba}(row + 1, col + 2) = R^{spa}(i, col2 + 1)^*$ 
28:    $R_{LD}^{abba}(row + 2, col + 2) = R^{spa}(i, col2 + 2)$ 
29:    $R_{LD}^{abba}(row + 3, col + 2) = R^{spa}(i, col2 + 3)^*$ 
30:    $R_{LD}^{abba}(row, col + 1) = R^{spa}(i, col2 + 1)$ 
31:    $R_{LD}^{abba}(row + 1, col + 1) = -R^{spa}(i, col2)^*$ 
32:    $R_{LD}^{abba}(row + 2, col + 1) = R^{spa}(i, col2 + 3)$ 
33:    $R_{LD}^{abba}(row + 3, col + 1) = -R^{spa}(i, col2 + 2)^*$ 
34:    $R_{LD}^{abba}(row, col + 3) = R^{spa}(i, col2 + 1)$ 
35:    $R_{LD}^{abba}(row + 1, col + 3) = -R^{spa}(i, col2)^*$ 
36:    $R_{LD}^{abba}(row + 2, col + 3) = R^{spa}(i, col2 + 3)$ 
37:    $R_{LD}^{abba}(row + 3, col + 3) = -R^{spa}(i, col2 + 2)^*$ 
38:    $col = col + 4, col2 = col2 + 4$ 
39:   endfor
40:    $col = 4n_s + 1, col2 = n_s + 1, row = row + 4$ 
41: endfor
42:  $R_{LD} = \begin{bmatrix} R_{LD}^{spa} & R^{div} \end{bmatrix}, Q_{LD} = \begin{bmatrix} Q_{LD}^{spa} & Q^{div} \end{bmatrix}$ 

```

## 6. Simulation results

To demonstrate the advantages of the codes presented in section 5 we compare the bit error rate (BER) performance of recent hybrid codes, employing 16-QAM modulation. In all cases, we have fixed the code rate to 3 symbols per channel use. The block length is fixed to  $L = 4$ . We remark that, besides better BER performance, the codes we have presented have lower receiver complexity, requiring between 4% and 12% fewer multiplications.

In Figure 7, we show the BER performance comparison between QR Group Receiver  $6 \times 6$  (Zhao & Dubey, 2005), STBC-VBLAST algorithm  $6 \times 6$  (2, 2, 3) (Mao et al., 2005), and ZF-SQRD LQOSTBC with  $n_R = 6, n_T = 6$  and  $n_A = 4$ .

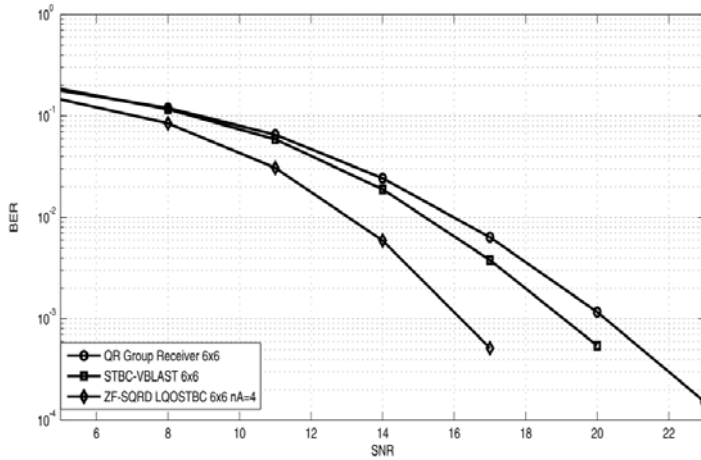


Fig. 7. BER vs. SNR of ZF-SQRD LQOSTBC, STBC-VBLAST  $6 \times 6$  (2, 2, 3) and QR Group Receiver  $6 \times 6$ .

Regarding ZF-SQRD LDSTBC, the block length is fixed to  $L = 2$ . In Figure 8, we show the BER performance comparison between QR Group Receiver  $6 \times 6$ , STBC-VBLAST  $6 \times 6$  (2, 2, 3), and ZF-SQRD LDSTBC with  $n_R = 6$ ,  $n_T = 6$  and  $n_B = 3$ .

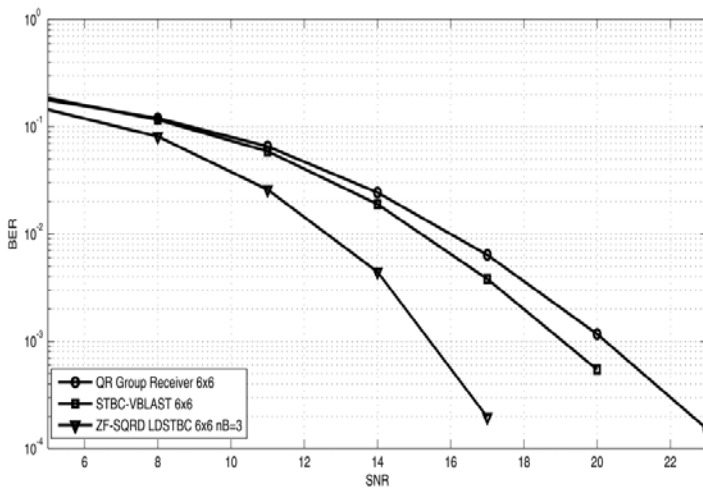


Fig. 8. BER vs. SNR of ZF-SQRD LDSTBC, STBC-VBLAST  $6 \times 6$  (2, 2, 3) and QR Group Receiver  $6 \times 6$ .

### 7. Conclusions

We have presented an overview of space-time block codes, with a focus on hybrid codes, and analyzed in some depth two hybrid MIMO space-time codes with arbitrary number of



STBC/ABBA and spatial layers, and a receiver algorithm with very low complexity. We have used the theory of linear dispersion codes to transform the original MIMO system to an equivalent system where the OSIC method for nulling and cancellation of the interference among layers can be applied.

## 8. Future Research

There are many open, interesting lines of research on hybrid codes. One is to carry out a theoretical analysis of their spectral efficiency versus diversity trade-off. It would also be interesting to explore a hardware implementation of a hybrid MIMO transceiver. Finally, as the performance limits of perfect space-time codes become well understood, hybrid codes remain an attractive alternative, although more rigorous and powerful construction and analysis techniques are required.

## 9. Acknowledgments

We thank the CONACYT research (grant 51332-Y) and Intel research grant INTEL-CERMIMO2008 and PROMEP for supporting this work.

## 10. References

- Alamouti S. M. (1998). A Simple Transmit Diversity Technique for Wireless Communications, *IEEE Journal on Selected Areas in Communications*, vol. 16, no. 8, October 1998, pp. 1451-1458, ISSN:0733-8716
- Arar, M. & Yongacoglu A. (2006) Efficient Detection Algorithm for  $2N \times 2N$  MIMO Systems Using Alamouti Code and QR Decomposition, *IEEE Communication Letters*, vol. 10, no. 12, December 2006, pp. 819-821, ISSN:1089-7798
- Berhuy G. & Oggier F. (2009). On the Existence of Perfect Space-Time Codes, *IEEE Transactions on Information Theory*, Vol. 55, No. 5, May 2009, pp. 2078-2082, ISSN: 0018-9448
- Biglieri E., Calderbank R., Constantinides A., Goldsmith A., Paulraj A., & Poor H. V. (2007). *MIMO Wireless Communications*, Cambridge University Press, ISBN: 978-0-521-87328-4, United Kingdom
- Cortez J., Bazdresch M., Torres D. & Parra-Michel R. (2007). An Efficient Detector for Non-Orthogonal Space-Time Block Codes with Receiver Antenna Selection, *Proceedings of the 18<sup>th</sup> IEEE International Symposium on Personal Indoor and Mobile Wireless Communications*, pp. 1-5, ISBN: 978-1-4244-1144-3, Athens, Greece, September 2007
- Cortez J., Bazdresch M., Torres D. & Parra-Michel R. (2008). Generalized ABBA-VBLAST Hybrid Space-Time Code for MIMO Wireless Communications, *Proceedings of the 9<sup>th</sup> IEEE International Workshop on Signal Processing Advances in Wireless Communications*, pp. 481-485, ISBN:978-1-4244-2045-2, Recife, Brazil, July 2008
- Dai L., Sfar S. & Letaief K. (2007). A Quasi-Orthogonal Group Space-Time Architecture to Achieve a Better Diversity-Multiplexing Tradeoff, *IEEE Transactions on Wireless Communications*, Vol. 6, No. 4, pp. 1295-1307, April 2007, ISSN: 1536-1284

- Foschini G. J. & Gans M. J. (1998). On Limits of Wireless Communications in a Fading Environment when Using Multiple Antennas. *Wireless Personal Communications*, Vol. 6, No. 3, March 1998, pp. 311-335, ISSN: 0929-6212
- Freitas W., Cavalcanti F. & Lopes R. (2006). Hybrid MIMO Transceiver Scheme with Antenna Allocation and Partial CSI at Transmitter, *Proceedings of the 17<sup>th</sup> Annual International Symposium on Personal Indoor and Mobile Radio Communications*, pp. 1-5, ISBN:1-4244-0329-4, Helsinki, Finland, September 2006
- Gesbert D., Shafi M., Shiu D.-S., Smith P. J. & Naguib A. (2003). From Theory to Practice: an Overview of MIMO Space-Time Coded Wireless Systems, *IEEE Journal on Selected Areas in Communications*, Vol. 21, No. 3, April 2003, pp. 281-302, ISSN: 0733-8716
- Golden G., Foschini G., Valenzuela R. & Wolniansky P. (1999). Detection Algorithm and Initial Laboratory Results Using VBLAST, *Electronic Letters*, Vol. 35, No. 1, January 1999, pp. 14-16, ISSN:0013-5194
- Hassibi B. & Hochwald B. (2002) High-rate Codes that are Linear in Space and Time, *IEEE Transactions on Information Theory*, vol. 48, no. 7, July 2002, pp. 1804-1824, ISSN:0018-9448
- Jafarkhani H. (2001). A Quasi-Orthogonal Space-Time Block Code. *IEEE Transactions on Communications* Vol. 49, No. 1, January 2001, pp. 1-4, ISSN: 0090-6778
- Kim H., Park H., Kim T. & Eo I., Performance Analysis of DSTTD System with Decision Feedback Detection, *Proceedings of IEEE International Conference on Acoustics, Speech and Signal Processing*, pp. 14-18, ISBN: 1-4244-0728-1, May 2006, Toulouse
- Kwak K., Kim J., Park B. & Hong D. (2005). Performance Analysis of DSTTD Based on Diversity-Multiplexing Trade-off, *61st IEEE Vehicular Technology Conference*, 2005, Vol. 2, pp. 1106-1109, 30 May-1 June 2005
- Longoria O., Sanchez A., Cortez J., Bazdresch M. & Parra-Michel R. (2007) Linear Dispersion Codes Generation from Hybrid STBC-VBLAST Architectures, *Proceedings of IEEE International Conference on Electrical and Electronics Engineering*, pp. 142-145, ISBN: 1-4244-1166-1, September 2007, Mexico
- Mao T. & Motani M. (2005) STBC-VBLAST for MIMO Wireless Communication Systems, *Proceedings of IEEE International Conference on Communications*, pp. 2266-2270, ISBN: 0-7803-8938-7, May 2005, Seoul
- Oggier F., Belfiore J.-C. & Viterbo E. (2007). Cyclic Division Algebras: A Tool for Space-Time Coding. *Foundations and Trends in Communications and Information Theory*, Vol. 4, No. 1, pp. 1-95, 2007, ISBN: 978-1-60198-050-2
- Paulraj A., Gore D. A., Nabar R. U. & Bölcskei H. (2004). An Overview of MIMO Communications-A Key to Gigabit Wireless. *Proceedings of the IEEE*, Vol. 92, No. 2, February 2004, pp. 198-218, ISSN: 0018-9219
- Pe M., Pham V., Mai L. & Yoon G. (2005). Low-complexity maximum-likelihood decoder for four-transmit-antenna quasi-orthogonal space-time block code, *IEEE Transactions on Communications*, vol. 53, no. 11, November 2005, pp. 1817-1821, ISSN: 0090-6778
- Tarokh V., Jafarkhani H. & Calderbank A. (1999). Space-Time Block Codes from Orthogonal Designs, *IEEE Transactions on Information Theory*, vol. 45, no. 5, July 1999, pp. 1456-1467, ISSN: 0018-9448
- Telatar I. (1999). Capacity of Multiple-Antenna Gaussian Channels. *European Transactions on Telecommunications*, Vol. 10, No. 6, February 1999, pp. 585-595, ISSN: 1120-3862.

- Tirkkonen O., Boariu A. & Hottinen A. (2000). Minimal Non-Orthogonality Rate 1 Space-Time Block Code for 3+ Tx Antennas, *Proceedings of the 6th International Symposium on Spread-Spectrum Technology and Applications*, New Jersey, USA, September 6-8, 2000
- Tse D. & Viswanath D. (2005), *Fundamentals of Wireless Communications*, Cambridge University Press, ISBN: 0521845270, England.
- Wubben D., Bohnke R., Rinas J., Kuhn V. & Kammeyer K. (2001). Efficient algorithm for decoding layered space-time codes, *IEE Electronic Letters*, vol. 37, no. 22, October 2001, pp. 1348-1350, ISSN: 0013-5194.
- Zhao L. & Dubey V. (2005). Detection Schemes for Space-Time Block Code and Spatial Multiplexing Combined System, *IEEE Communication Letters*, vol. 9, no. 1, January 2005, pp. 49-51, ISSN: 1089-7798
- Zheng L. & Tse D. (2003) Diversity and Multiplexing: Fundamental TradeOff in Multiple Antenna Channels, *IEEE Transactions on Information Theory*, vol. 49, no. 5, May 2003, pp. 1073-1096, ISSN: 0018-9448





## **Mobile and Wireless Communications Physical Layer Development and Implementation**

Edited by Salma Ait Fares and Fumiyuki Adachi

ISBN 978-953-307-043-8

Hard cover, 290 pages

**Publisher** InTech

**Published online** 01, January, 2010

**Published in print edition** January, 2010

Mobile and Wireless Communications have been one of the major revolutions of the late twentieth century. We are witnessing a very fast growth in these technologies where mobile and wireless communications have become so ubiquitous in our society and indispensable for our daily lives. The relentless demand for higher data rates with better quality of services to comply with state-of-the-art applications has revolutionized the wireless communication field and led to the emergence of new technologies such as Bluetooth, WiFi, Wimax, Ultra wideband, OFDMA. Moreover, the market tendency confirms that this revolution is not ready to stop in the foreseen future. Mobile and wireless communications applications cover diverse areas including entertainment, industrialist, biomedical, medicine, safety and security, and others, which definitely are improving our daily life. Wireless communication network is a multidisciplinary field addressing different aspects ranging from theoretical analysis, system architecture design, and hardware and software implementations. While different new applications are requiring higher data rates and better quality of service and prolonging the mobile battery life, new development and advanced research studies and systems and circuits designs are necessary to keep pace with the market requirements. This book covers the most advanced research and development topics in mobile and wireless communication networks. It is divided into two parts with a total of thirty-four stand-alone chapters covering various areas of wireless communications of special topics including: physical layer and network layer, access methods and scheduling, techniques and technologies, antenna and amplifier design, integrated circuit design, applications and systems. These chapters present advanced novel and cutting-edge results and development related to wireless communication offering the readers the opportunity to enrich their knowledge in specific topics as well as to explore the whole field of rapidly emerging mobile and wireless networks. We hope that this book will be useful for students, researchers and practitioners in their research studies.

### **How to reference**

In order to correctly reference this scholarly work, feel free to copy and paste the following:

Joaquin Cortez and Miguel Bazdresch (2010). High-Rate, Reliable Communications with Hybrid Space-Time Codes, Mobile and Wireless Communications Physical Layer Development and Implementation, Salma Ait Fares and Fumiyuki Adachi (Ed.), ISBN: 978-953-307-043-8, InTech, Available from: <http://www.intechopen.com/books/mobile-and-wireless-communications-physical-layer-development-and-implementation/high-rate-reliable-communications-with-hybrid-space-time-codes>

**INTECH**  
open science | open minds

**InTech Europe**

University Campus STeP Ri  
Slavka Krautzeka 83/A  
51000 Rijeka, Croatia  
Phone: +385 (51) 770 447  
Fax: +385 (51) 686 166  
[www.intechopen.com](http://www.intechopen.com)

**InTech China**

Unit 405, Office Block, Hotel Equatorial Shanghai  
No.65, Yan An Road (West), Shanghai, 200040, China  
中国上海市延安西路65号上海国际贵都大饭店办公楼405单元  
Phone: +86-21-62489820  
Fax: +86-21-62489821